

Electronic supplementary information

Suppressing singlet oxygen generation in lithium-oxygen batteries with redox mediators

Zhuojian Liang, Qingli Zou, Jing Xie and Yi-Chun Lu*

Electrochemical Energy and Interfaces Laboratory, Department of Mechanical and Automation Engineering, The Chinese University of Hong Kong, Hong Kong, SAR 999077, China.

* E-mail: yichunlu@mae.cuhk.edu.hk

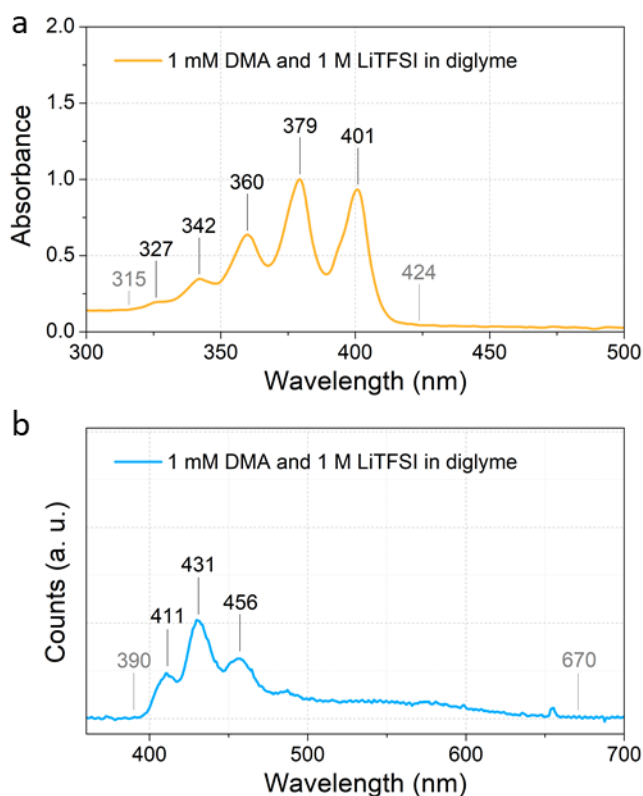


Figure S1. UV-Vis spectra of DMA. (a) Absorbance spectrum; (b) fluorescence spectrum.

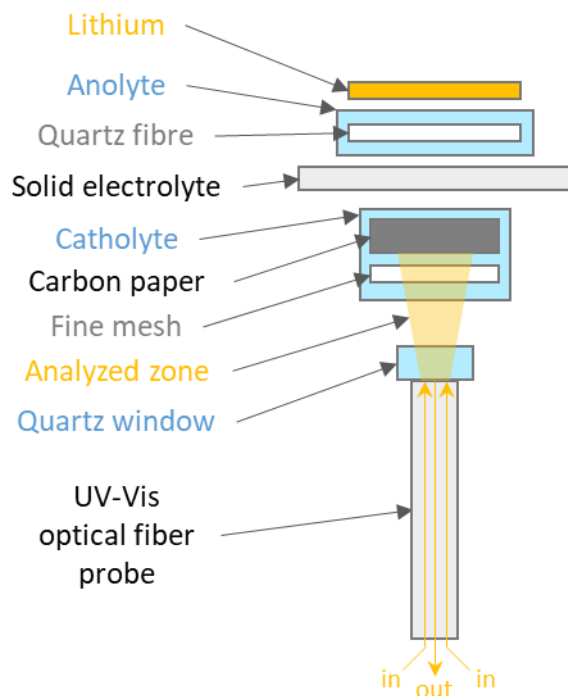


Figure S2. Layout of the components inside the custom-designed operando UV-Vis spectroscopy cell. From top to bottom is: lithium disk (\varnothing 16 mm), quartz fibre disk (\varnothing 14 mm) soaked with 90 μ l 0.1 M LiTFSI in diglyme, Li^+ -conducting solid electrolyte (LAGP, see Experimental methods for synthesis procedure) disk (\varnothing 19 mm), carbon paper disk (H2315, \varnothing 10 mm) and stainless steel mesh (\varnothing 10 mm) soaked with 20 μ l 20 mM DMA and 1 M LiTFSI in diglyme, quartz window (\varnothing 4 mm), optical fiber probe. Cell components are placed in contact, while they are drawn apart here for clarity.

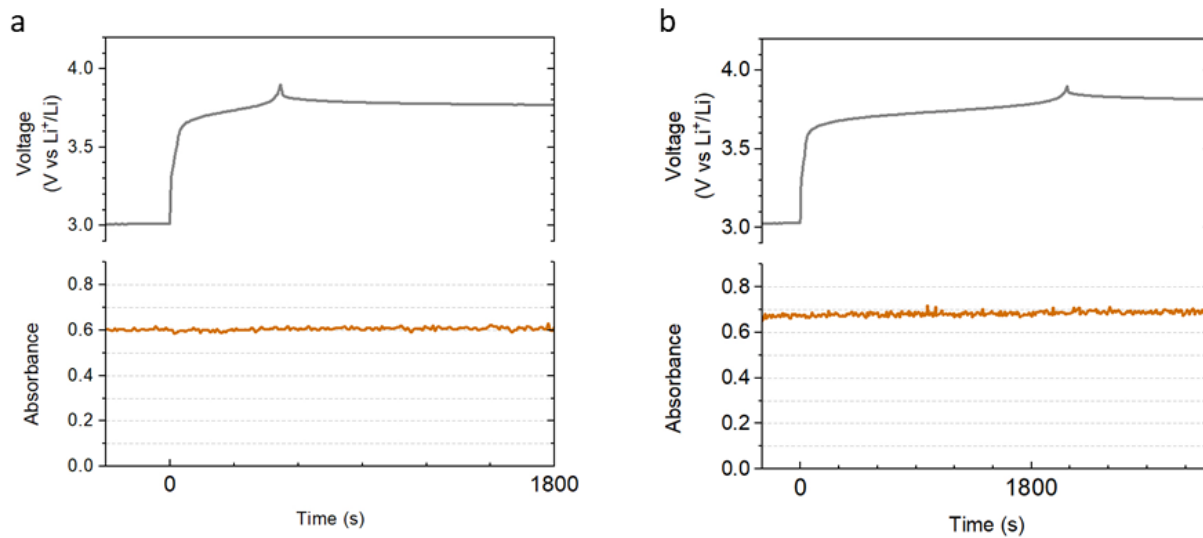


Figure S3. *operando* UV-Vis absorbance at 379 nm during oxidation of (a) 2 mM TEMPO and (b) 10 mM TEMPO. The spectra were recorded in 2 mM TEMPO – 20 mM DMA - 1 M LiTFSI - diglyme electrolyte and 10 mM TEMPO - 20 mM DMA - 1 M LiTFSI - diglyme electrolyte. This absorbance rise in panel b is equivalent to absorbance by 0.6 mM DMA concentration.

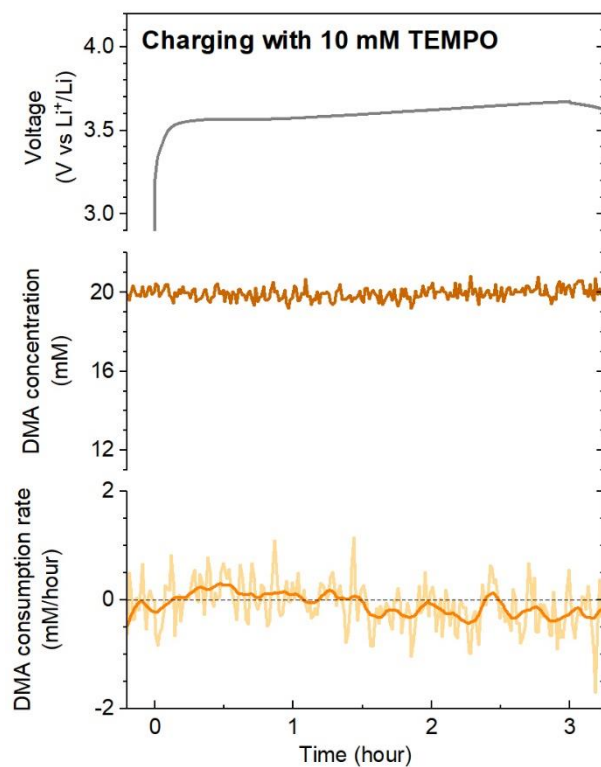


Figure S4. Operando UV-Vis spectroscopy characterizing DMA consumption during charge with 10 mM TEMPO. Overall, the detected DMA consumption throughout charging is negligible. The background contribution of 10 mM TEMPO during charging is shown in Figure S3.

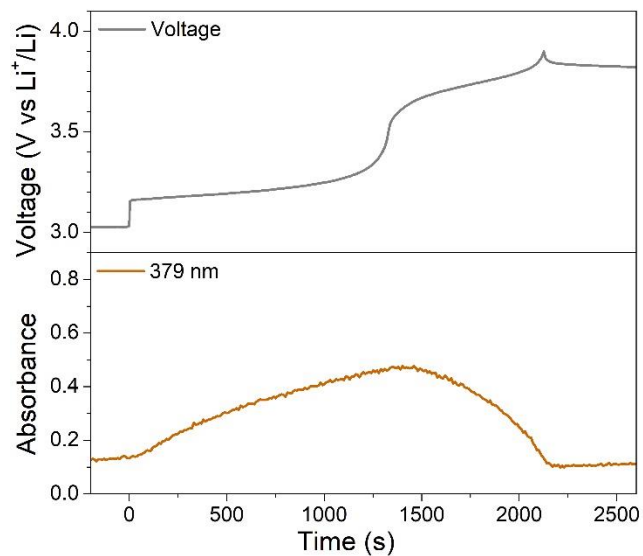


Figure S5. *operando* UV-Vis absorbance at 379 nm during oxidation of LiI. The spectrum was recorded in 10 mM LiI - 1 M LiTFSI - diglyme electrolyte.

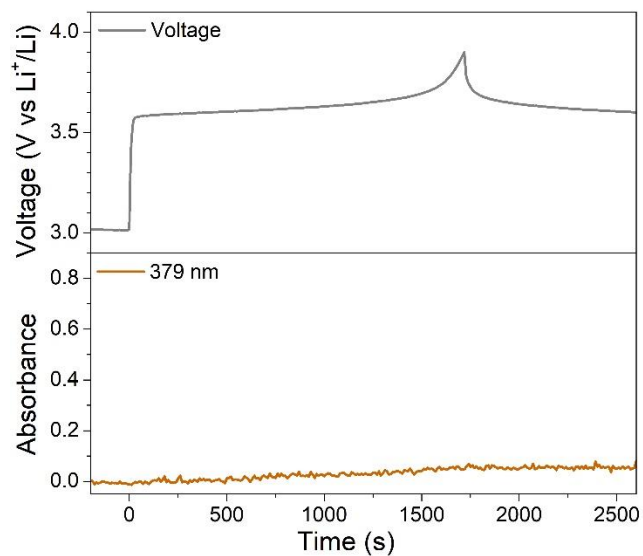


Figure S6. *operando* UV-Vis absorbance at 379 nm during oxidation of LiBr. The spectrum was recorded in 10 mM LiBr - 1 M LiTFSI - diglyme electrolyte.

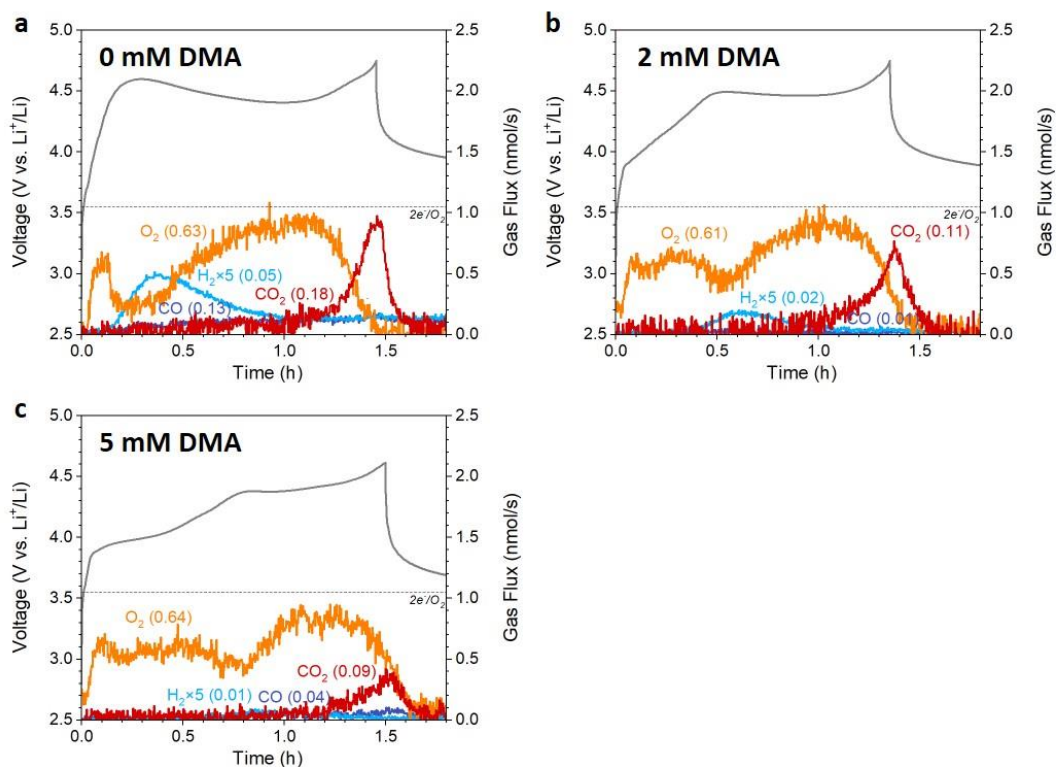


Figure S7. Voltage and gas evolution profiles during charging with various concentrations of DMA in the electrolyte.

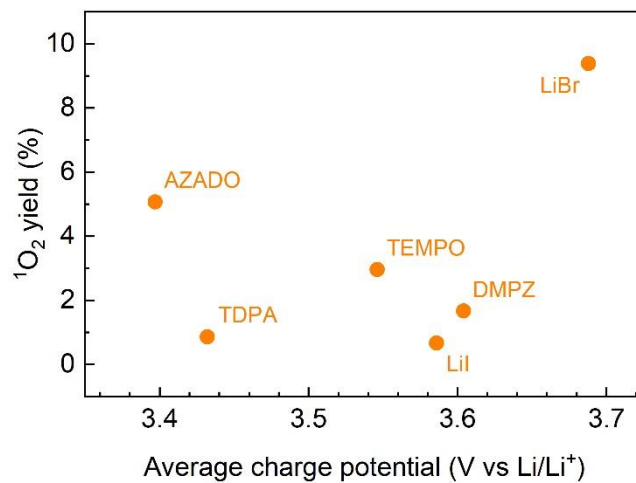


Figure S8. A comparison of the ¹O₂ yield and average charge potential of the six redox mediators investigated in this work.

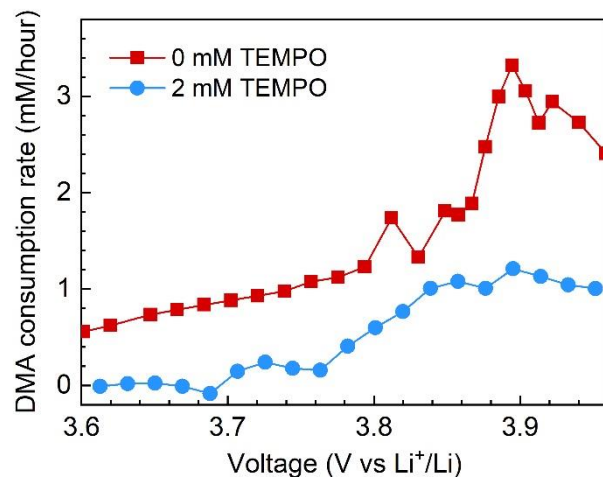


Figure S9. A comparison of the DMA consumption rates at various potentials when different TEMPO concentrations are used in Figure 2. For both cells, ¹O₂ generation rate is not a monotone function of voltage.

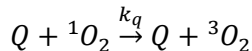
Table S1 Absorbance of species in the electrolyte

Species	Absorbance at 379 nm ($\text{mM}^{-1} \text{mm}^{-1}$)	Electrolyte	Percentage of absorbance by DMA in the electrolyte
DMA	1.040	20 mM DMA	100.00%
TEMPO	0.0051	20 mM DMA + 2 mM TEMPO	99.95%
LiI	0.0027	20 mM DMA + 10 mM LiI	99.87%
LiBr	0.0000	20 mM DMA + 10 mM LiBr	100.00%

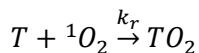
Supplementary Note 1

Three rate constants are used in literature to describe the reactivity of a molecule with $^1\text{O}_2$:

- (1) Reversible $^1\text{O}_2$ quenching rate constants k_q of a molecule, e.g. a quencher Q:



- (2) Irreversible $^1\text{O}_2$ reaction rate constants k_r of a molecule, e.g. a trap T:



- (3) Total rate constant k_t of a molecule:

$$k_t = k_q + k_r$$

An ideal $^1\text{O}_2$ quencher displays $k_r = 0$, while an ideal $^1\text{O}_2$ trap displays $k_q = 0$.

To quantitatively describe the $^1\text{O}_2$ suppression capability of mediators, we define the $^1\text{O}_2$ suppression rate constants k_{sup} of the redox mediators as the equivalent k_q if the mediators were to quench $^1\text{O}_2$ like quenchers, which can be used to compare with the $^1\text{O}_2$ quenching rate constant k_q of a quencher.

We estimate these rate constants relative to the total reaction rate constant of DMA $k_{t, \text{DMA}}$.¹ Since $k_{t, \text{DMA}}$ in the diglyme-based electrolyte we are using has not been reported, we use an average of the values reported in four solvents (ranging from $2.1 \times 10^7 \text{ M}^{-1} \text{ s}^{-1}$ to $9.3 \times 10^7 \text{ M}^{-1} \text{ s}^{-1}$), i.e. $6.75 \times 10^7 \text{ M}^{-1} \text{ s}^{-1}$.²

In the cell without mediators, we assume that most of $^1\text{O}_2$ react with DMA after generation, i.e. negligible amount of $^1\text{O}_2$ has reacted with electrolyte or decayed itself, which is a reasonable assumption given the high DMA concentration we used and its fast reaction kinetics. Then the amount of DMA- O_2 generation without mediators equals to the total amount of $^1\text{O}_2$ generation:

$$n_{\text{DMA-O}_2, \text{w/o RM}} = n_{1\text{O}_2} \quad (1)$$

In the cell with mediators, DMA and the virtual quenchers (mediators) compete for $^1\text{O}_2$, the amount of DMA- O_2 with mediators is:

$$n_{\text{DMA-O}_2, \text{w/ RM}} = n_{1\text{O}_2} * \frac{k_{t, \text{DMA}} * c_{\text{DMA}}}{k_{t, \text{DMA}} * c_{\text{DMA}} + k_{\text{sup}} * c_{\text{RM}}} \quad (2)$$

Where c_{DMA} and c_{RM} are the concentrations of DMA and mediators, respectively.

From equations (1) and (2), the $^1\text{O}_2$ suppression rate constants of the redox mediators k_{sup} can be obtained:

$$k_{\text{sup}} = \left(\frac{n_{\text{DMA-O}_2, \text{w/o RM}}}{n_{\text{DMA-O}_2, \text{w/ RM}}} - 1 \right) * \frac{c_{\text{DMA}}}{c_{\text{RM}}} * k_{t, \text{DMA}} \quad (3)$$

Supplementary Note 2

The total reaction rate (including irreversible decomposition reaction rate and reversible quenching reaction rate) constants k_t between mediators and $^1\text{O}_2$ are plotted together with k_{sup} :

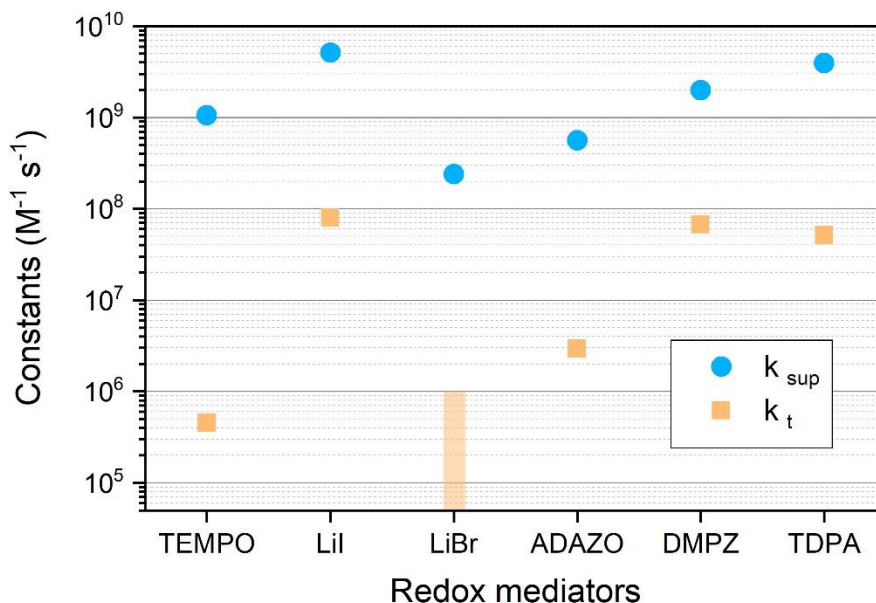


Figure S10. $^1\text{O}_2$ suppression rate constants of the redox mediators k_{sup} estimated from the DMA- O_2 quantification data, and the total reaction rate constants of mediators k_t . k_t of LiI and TEMPO are taken from literature.^{3, 4} LiBr was reported to show no quenching effect or a rate constant $< 10^6 \text{ M}^{-1} \text{s}^{-1}$.³ We measured k_t of TDPA, DMPZ and ADAZO following the method described below.

Similar to the estimation of k_{sup} (equation 3), k_t of TDPA, DMPZ and ADAZO are estimated relative to $k_{t, \text{DMA}}$:

$$k_t = \left(\frac{n_{\text{DMA}-\text{O}_2, \text{w/o RM}}}{n_{\text{DMA}-\text{O}_2, \text{w/ RM}}} - 1 \right) * \frac{c_{\text{DMA}}}{c_{\text{RM}}} * k_{t, \text{DMA}} \quad (4)$$

An excess amount of KO_2 powder is added into solutions of 0.2 M TBAClO_4 and 1 mM DMA and 1 M LiTFSI in diglyme, without or with 1 mM RM (RM=TDPA, DMPZ or ADAZO). Upon mixing of the powder with the solutions, Li^+ catalyses KO_2 disproportionation, which generates singlet oxygen and is promoted by TBA^+ .⁵ After reaction, the amounts of DMA consumption without and with mediators (Figure S8) determined using UV-Vis spectrometry at 379 nm (with the absorbances of mediators subtracted) are used to estimate k_t according to equation (4). This *ex situ* experiment may not accurately determine the k_t of these mediators; however, it gives a reasonable estimation of their order of magnitude.

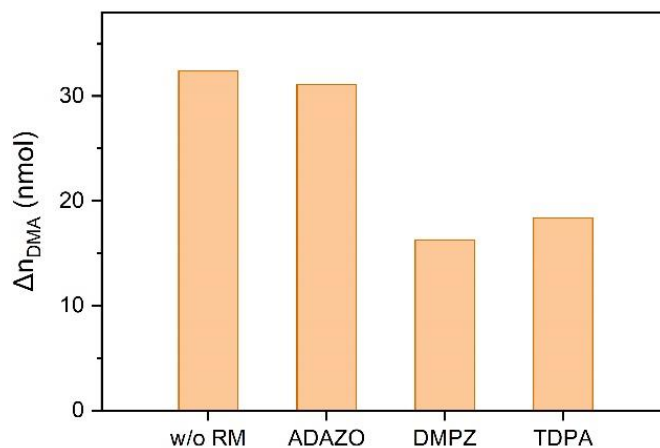


Figure S11. The amounts of DMA consumption without and with mediators after reaction.

Reference:

1. J. Wandt, P. Jakes, J. Granwehr, H. A. Gasteiger and R. A. Eichel, *Angew. Chem. Int. Ed.*, 2016, **128**, 7006-7009.
2. G. Günther S, E. Lemp M and A. L. Zanocco, *Boletín de la Sociedad Chilena de Química*, 2000, **45**, 637-644.
3. I. Rosenthal and A. Frimer, *Photochemistry and Photobiology*, 1976, **23**, 209-211.
4. F. Wilkinson and J. G. Brummer, *Journal of Physical and Chemical Reference Data*, 1981, **10**, 809-999.
5. E. Mourad, Y. K. Petit, R. Spezia, A. Samojlov, F. F. Summa, C. Prehal, C. Leypold, N. Mahne, C. Slugovc, O. Fontaine, S. Brutti and S. A. Freunberger, *Energy Environ. Sci.*, 2019, **12**, 2559-2568.